Original Paper

Landslides (2025) 22:2573–2584
DOI 10.1007/s10346-025-02538-3
Received: 14 December 2023
Accepted: 8 May 2025
Published online: 22 May 2025
The Author(s) 2025

Karel Šilhán · Ivan Ružek

First dendrogeomorphological dating of DSGSD: specificity of the reconstruction

Abstract Globally, one of the most widespread types of slope deformation is DSGSD (deep-seated gravitational slope deformation), which typically takes tens of thousands of years to develop, but can also be catastrophically reactivated and may represent a recent natural hazard. Knowledge of their past evolution is based mostly on absolute dating of old whereas recent evolution can be covered by appropriate monitoring. Bridging these two time periods is currently a major challenge. This study thus presents unique dating of DSGSD evolution using dendrogeomorphic (tree-ring-based) methods over the last 60 years. The uniqueness of the study also lies in the origin of DSGSD, which was anthropogenically induced through deep lignite mining that began in 1962. Tree-ring-based data from 71 disturbed trees (*Fagus sylvatica* L. and *Larix decidua* Mill.) revealed the specific effects of DSGSD movements on the growth of both tree species, which are usable in future research. At the same time, the obtained chronology of movements revealed the occurrence of initial failure of DSGSD and their subsequent cessation, except for one part of the studied slope, in which there is a simultaneous recovery of movements. The dendrogeomorphic analysis confirmed the generally assumed evolution of DSGSD but in a very limited time period, which may be related to the anthropogenic influence on its formation. The research was complemented by an analysis of the dynamics of post-failure evolution of landforms based on anatomical data from exposed tree roots. The results suggest rapid erosional modelling of the newly formed DSGSD.

Keywords Dendrogeomorphology · DSGSD · Anthropogenic impact · Growth disturbance · Erosion

Introduction

Deep-seated gravitational slope deformation (DSGSD; Agliardi et al. 2001) is a significant type of disruption of slopes and entire mountain ridges, which breaks them to great depths, significantly modelling their morphology, but also reducing their stability, which can lead to catastrophic collapses (Dramis and Sorriso-Valvo 1994; Shroder et al. 2011). Thus, it is potentially a significant natural hazard (Chigira et al. 2010) that can negatively affect human infrastructure (Ambrosi and Crosta 2006), as well as cause loss of life.

The recent emergence of entirely new initial failures is rarely described (Blair 1994; Jibson et al. 2004). Initial failures tend to be triggered during strong earthquakes (Moro et al. 2007). However, the origin of most DSGSDs is assumed (Pánek and Klimeš 2016) to be in two periods, with the first following deglaciation (18–10 ka CE) and the origin of the second group in unglaciated areas possibly even older (Hughes et al. 2013; Pánek et al. 2018). Therefore, radiometric absolute dating methods need to be applied to determine the age of these initial failures (Bigot-Cormier et al. 2005; Hermanns et al. 2013; Zerathe et al. 2013), but they show considerable variability in the resulting dates (Pánek 2015). The actual post-failure evolution of DSGSDs is characterized by long-term slow creep (up to 0.1 mm.year^{-1}) with occasional accelerations of motion (Klimeš et al. 2012). However, the question of the chronological evolution is quite the least studied compared to morphometry, spatial distribution or the influence of geological structure (Crosta et al. 2013).

The origin and development of DSGSD is completely dominated by natural influences and (to our knowledge) the initial failure and subsequent development due to anthropogenic interference has not been described. In this study, however, we present an area where the origin of DSGSD was driven entirely by anthropogenic activity and whose initial failure is only a few decades old. This situation thus allows a unique exploration of the spatio-temporal evolution of this type of slope deformation. However, reconstruction using radiometric techniques is not possible in this case due to the low age of the deformation. Dendrogeomorphic methods (Alestalo 1971) were used for spatio-temporal reconstruction of DSGSD for the very first time. Their previous use for DSGSD dating has not been possible because of high ages or too small movements (one of the limitations of dendrogeomorphology; Corona et al. 2014). The only exceptions are the attempts by Fantucci and Sorriso-Valvo (1999) or Leonelli et al. (2020) who used tree-ring based approaches to analyze not directly DSGSD movements, but movements of other slope processes that occurred on the DSGSD surface (e.g., shallow creep). Thus, direct dating of DSGSD movements through dendrogeomorphic methods has not yet been implemented.

In general, dendrogeomorphic methods are currently considered the most accurate method for absolute dating of slope processes in environments with woody vegetation capable of forming an annual increment in the form of a tree ring (Stoffel et al. 2013a). The method can date events up to several hundred years old (Zhang et al. 2019) with precision down to a season or several months (Clague and Souther 1982). In DSGSD research, the chronological resolution of reactivation phases is quite extraordinary. The tree-ring-based approach relies on dendrochronological dating of growth disturbances (GD) in tree-ring series that are induced by the action of a geomorphic process (Shroder 1978). In the case of slow slope processes (landsliding, creep), this most often involves the formation of reaction wood on one side of the trunk in response to its lean (Westing 1965) or abrupt growth suppression as a growth response to damage to the tree root system due to subsurface movements (Stoffel and Bollschweiler 2008). However, an essential condition for the effective use of this methodological apparatus is that the magnitude of the movements studied is sufficient (they must be able to affect tree growth; Lopez Saez et al. 2012). In the case of old long-term and very small creep movements within the DSGSD, there was

practically no possibility of dating them dendrogeomorphically. The margins of fresh cracks or major and minor scarps after initial failure are subject to erosion (also in the case of DSGSD) and smoothening of the original morphology. Dendrogeomorphology can date these erosional processes by studying the anatomical structure of exposed tree roots (Vandekerckhove et al. 2001).

Based on the above, it is clear that dendrogeomorphic dating of DSGSD is a major challenge and its success rate can be increased when applied to young, dynamically developing forms, which are, however, extremely rare. Thus, this study not only (i) presents a uniquely young DSGSD with an age of several decades, which is moreover anthropogenically induced, but (ii) also its spatio-temporal reconstruction using dendrogeomorphic methods. This combination is unique in the context of DSGSD research worldwide. The tree-ring based reconstruction focused not only on the spatio-temporal analysis of the distribution of the sub-movements, but also on (iii) the analysis and quantification of the erosional evolution of the edges of fresh cracks and ditches within the studied DSGSD. This paper also tries to describe the specifics of the tree-ring based approach in the analysis of this specific phenomenon.

Study area

The study site (48.71° N and 18.66° E; Fig. 1A) is located in the Upper Nitra region in Central Slovakia, specifically on the western slope of the Vtáčnik mountain ridge east of the village Cígeľ. The upper part of the ridge (and the study site) and the lower parts of the slopes are formed by alternating lava flows, pyroclastics and volcanic breccias. These volcanic complexes are underlain by softer complexes of Neogene (Baden) sediments (siltstones, sandstones, siltstones) interbedded with brown coal seams (Šimon et al. 1997). The Baden seams, rich in lignite, are intensively mined underground. The depth of extraction is mainly between 200 and 250 m, and the thickness of the lignite seams at this depth varies between approximately 3 and 30 m. Less thick brown coal seams of between approximately 2 and 9 m are found at various depths below the surface (120–510 m) (Czikhardt et al. 2017). The combination of a suitable geological structure (solid volcanic complexes in the overlying soft Neogene sediments) combined with intensive underground mining (Fig. 1C) has triggered landslide movements on the slopes and subsidence in the flatter parts of the terrain (Němčok 1982). This has created a regional anthropogenically induced natural hazard negatively

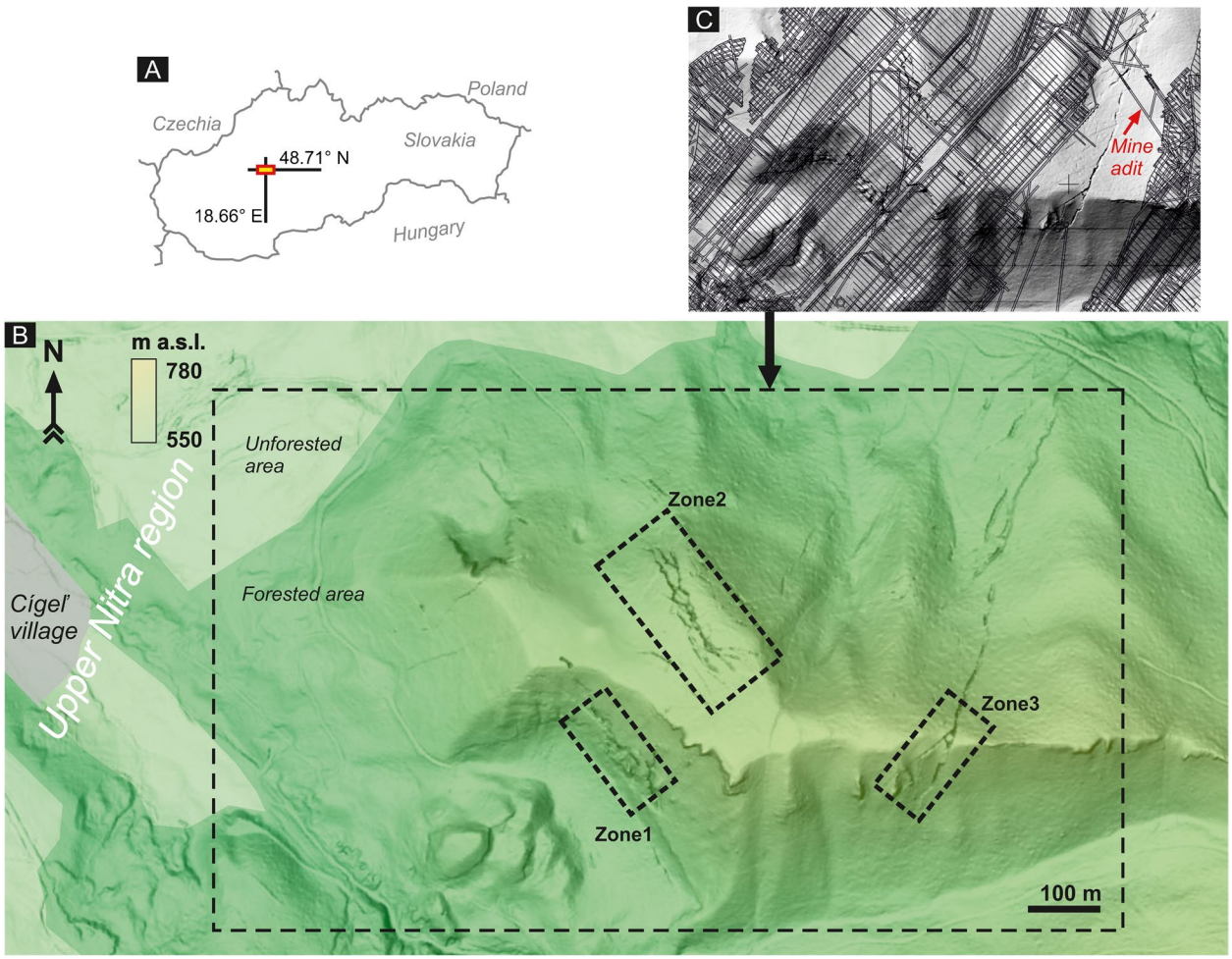


Fig. 1 Position of the study site within the Slovak Republic (**A**) and its detailed morphology on DEM (source: Digital elevation model [online]. Bratislava: State Geological Institute of Dionýz Štúr, 2009. Available from: http://apl.geology.sk/dmr) (**B**). **C** Spatial distribution of mine tunnels (black lines) under the site of interest

affecting the local infrastructure (Czikhardt et al. 2017). The beginning of underground mining started in 1962 (Cigel mine) and the largest volume of extracted material was in the late 1970 s and 1980 s (over 2 million tonnes of coal per year; Čičmanec et al. 2009). Mining is currently no longer active.

The climatic conditions of the study area can be characterized as moderately warm, moderately humid. The average annual temperature varies between 6 and 8 °C, with the average temperature in July (the warmest month) being 14–17 °C and the average temperature in January (the coldest month) being between − 3 and − 4 °C. The average annual rainfall is 650–800 mm and the number of days with rain is 100–120. Snow cover occurs for 45 to 75 days a year (Bochníček et al. 2015). In terms of real vegetation in the study area, beech forests in the foothills dominate with a dominant representation of *Fagus sylvatica* L. Enclaves of warm-loving oak forests with *Quercus petraea* (Matt.) Liebl. with a rich scrub vegetation grow on the rocky south-oriented outcrops. In the northern part of the territory are non-native monocultures of *Larix decidua* Mill.

The locality of interest itself is a mountain ridge in E–W direction, starting from the main ridge Vtáčnik. The area of the investigated site was about 0.2 km^2 with a maximum length of 600 m and a maximum width of 500 m. The inclination of the open cracks (up to purely vertical direction) reaches the maximum slope. The depth of the shear surfaces can be expected to be at least several tens of meters. The DSGSD affects this entire sub-ridge on its northern and southern slopes (Fig. 1B). Morphologically, DSGSD is manifested by typical forms such as blocks subsiding by several meters with open trenches (Fig. 2A), major and minor steps on slopes and flatter areas (Fig. 2B), open tension cracks (Fig. 2C) or partially open tension trenches (Fig. 2). Within the entire DSGSD, three defined sub-zones (morphogenetic units) have been studied in detail (Fig. 3A). Zone1 is located on the southern slope of the ridge and is characterized by two to three parallel open fissures/ditches in a contouring direction. The width of the opening reaches up to 3 m at the top (Fig. 3B). Zone2 is localized on the northern part of the ridge (Fig. 3A) and lies partly on its flatter watershed part. In this part, a system of subsiding blocks separated by interconnected open cracks and trenches (Fig. 3D) is developed, whose orientation is both in the direction of slope and contour. This whole part of the slope shows signs of a significant stage of block disintegration. Zone3 represents a belt along an extensive open crack across the entire ridge in the N–S direction. The crack splits into two branches on the southern part of the ridge. Maximum subsidence along the crack is at the top of the ridge and reaches 8–9 m here (Fig. 3C). The two branches of the crack on the southern part of the slope gradually decrease in width from about 5 to 1 m. At the lower extension value, the upper part of the crack is still covered by tree root systems (Fig. 2D).

Methods

Field procedures

The study site was first geomorphically mapped (Fig. 3) with a focus on the spatial distribution of the main morphological forms (open cracks and trenches, scarps of various heights, subsided blocks) based on LiDAR-based DEM and GNSS devices. Subsequently, trees growing in the immediate vicinity of these forms were sampled. The sampling design was developed to include only trees that could clearly be expected to have their growth impacts due to DSGSD movement. At the edges of open trenches and fresh scarps, trees with leaning trunks (Fig. 4A) due to subsidence or sprawl and trees that had visibly damaged

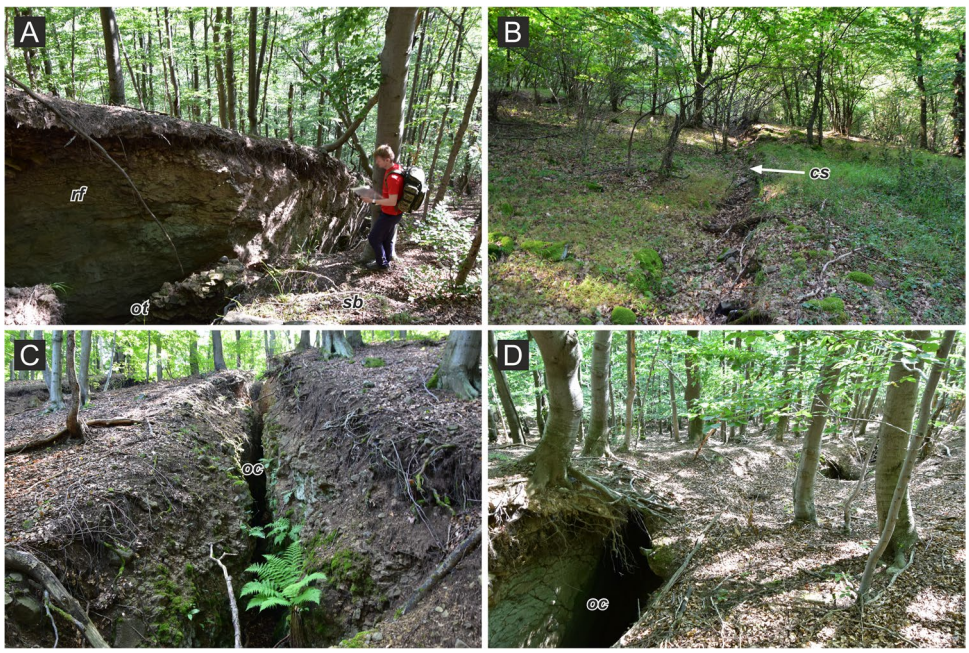


Fig. 2 Typical morphological features of the study area associated with the presence of DSGSD. **A** View of the exposed rock face above the subsided sub-block separated by an open trench. **B** Minor scarp resulting from subsidence of the block above. **C** Open cracks with apparent erosional remodelling of the upper margins. **D** Partially open crack overlain at the top by the original root system of *F. sylvatica* individuals

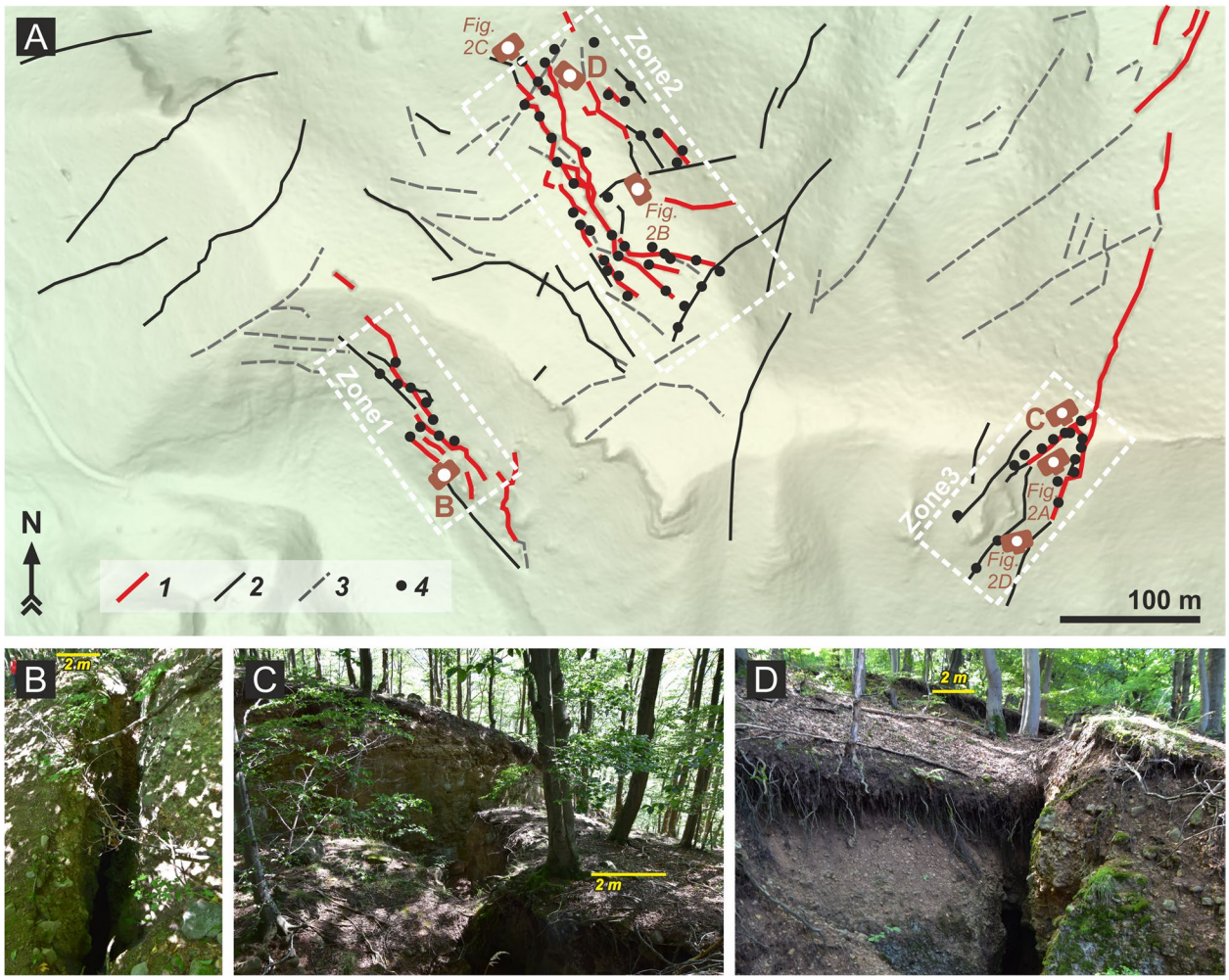


Fig. 3 Detailed morphology of the studied slopes affected by DSGSD movements. **A** Spatial distribution of open cracks and trenches (1), major scarps (2), minor scarps (3), and sampled trees (4) including the position of the three subzones studied. **B** Open crack on the slope in Zone1. **C** View of the exposed part of the rock outcrop above the subsidence block in Zone2. **D** Subsidence and rotated blocks in Zone3

roots (Fig. 4B) were sampled. At the edges of these forms with visible erosion processes, samples (approximately 2-cm-long cross-sections) were taken from exposed tree roots (Fig. 4). The perpendicular distance of each sample to the ground (current form surface) was measured to the nearest 1 cm. Specimens of *F. sylvatica* and *L. decidua* were sampled. The position of each sampled tree was recorded using a GNSS device. In addition to disturbed trees, 20 trees growing outside the influence of the studied processes but in the same microclimatic conditions were sampled for the construction of a reference chronology.

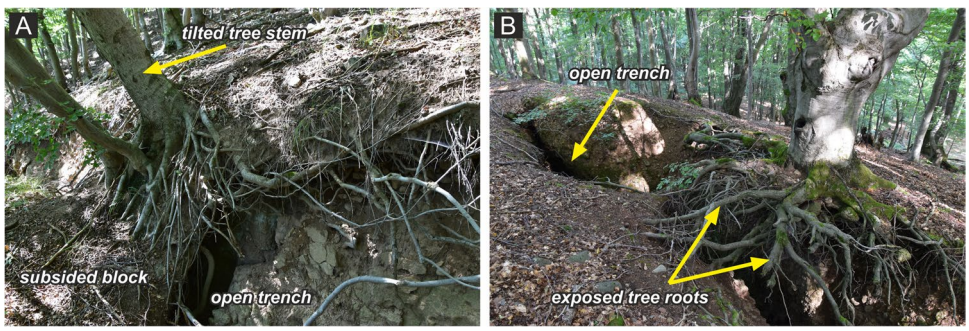


Fig. 4 Typical morphological conditions around sampled trees and roots. **A** A leaning *F. sylvatica* individual on a partial scarp with a visibly damaged root system. **B** An *F. sylvatica* individual growing on the edge of an open trench with exposed roots that allowed quantification of the erosion rate

Laboratory procedures

All increment cores were processed according to standard procedures used in the study of slope processes (Stoffel and Bollschweiler 2008; Šilhán 2020). Cores were air-dried, glued into woody supports and their surface was cut using a core-microtome (Gärtner et al. 2014). The surface of the samples was then treated with white chalk and all samples were scanned at 2400 dpi resolution. Tree-ring widths were measured in CooRecorder (Maxwell and Larsson 2021) to the nearest 0.01 mm. Reference chronologies were constructed in Arstan (Cook 1983). Any false or missing tree rings were identified by cross-dating of increment curves from disturbed trees against reference chronology in the program CDendro (Maxwell and Larsson 2021). The quality of the cross-dating was checked using the program Cofecha (Holmes 1983). Cross-sections from roots were prepared using a G.S.L.1 microtome (Gärtner and Nievergelt 2010), and these were subsequently chemically processed in a standard manner (Schweingruber 1978). Each microcut was treated with sodium hypochlorite, dehydrated with 50, 70, and 96% alcohol series, treated with Diasolv and mounted to slides with Canada balsam. Subsequently, the microcut specimens were placed in an oven for 12 h at 60 °C. The finished microcuts were then photographed at × 50 magnification and the vessel lumen area (VLA) was measured in WinCELL.

After chronological corrections, slope processed-induced GDs were identified from the increment curves and on the prepared increment cores surface. Attention was focused on the occurrence of reaction wood (compression type in the case of *L. decidua*, occurring on the underside of leaning trunks; tension type in the case of *F. sylvatica*, occurring on the upper side of leaning trunks; Fig. 5A; Timell 1986) and abrupt growth suppression, which was calculated as the percentage decrease in tree-ring width compared to the average of the four previous tree-rings (Schweingruber et al. 1990). The percentage decrease in tree-ring width was also used as a value for the intensity of abrupt growth suppression (Fig. 5B). Reaction wood was identified on the surface of cores treated with microtome under stereoscope. TRDs were not considered because the trees were not damaged and *F. sylvatica* does not form this type of growth disturbance. The moment of root exposure due to erosion processes was detected by a sharp decrease in VLA (up to 50%), which is a well-known response of tree roots to their exposure (Gärtner 2007; Rubiales 2008). Only GDs present in disturbed trees and absent in reference trees were considered to be the result of geomorphic processes.

The whole study area was divided into three morphogenetic units (Zones 1, 2, and 3) and a separate movement chronology was constructed for each of them, which is an effective tool for efficient extraction of the geomorphic signal and minimization of noise (Šilhán et al. 2022). For each zone, all GDs were chronologically summarized and activity was expressed using a standard event-response (I_t) index, which expresses the percentage of trees containing GDs in a given year out of all sampled trees that were alive in that year (Shroder 1978; Butler et al. 1987). The threshold for defining an event was chosen as 5% based on recommendations from Corona et al. (2014) and Stoffel et al. (2013a) with respect to

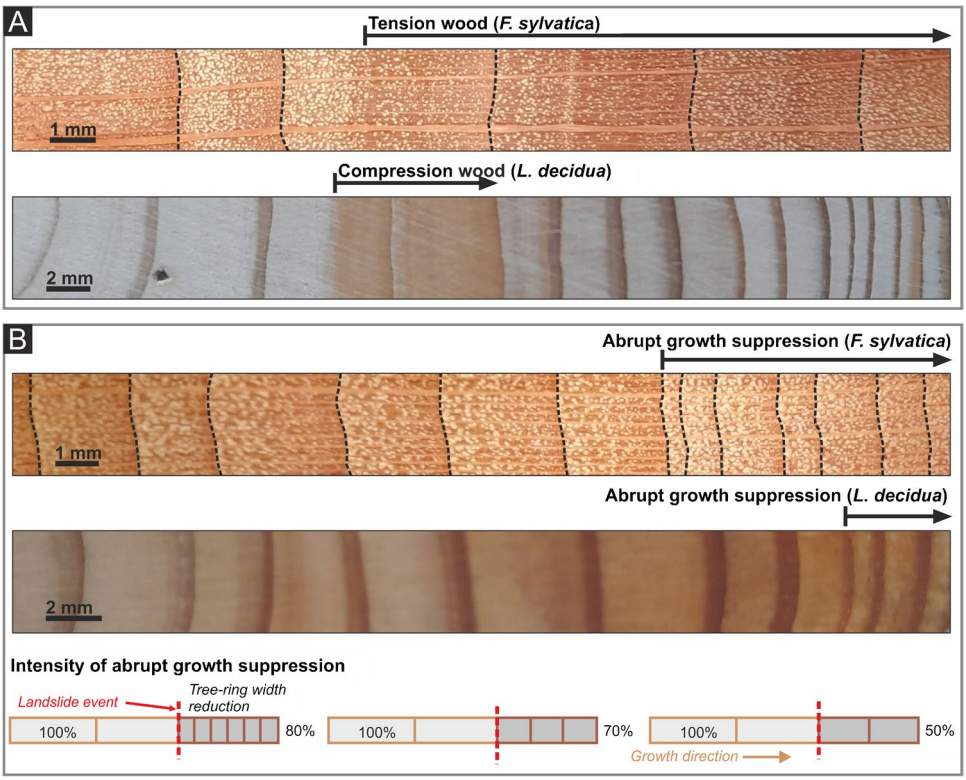


Fig. 5 Growth perturbations used for dating DSGSD movements. **A** Tension (in the case of *F. sylvatica*) and compression (in the case of *L. decidua*) reaction wood types. **B** Abrupt growth suppression on samples from both tree species, including a scheme for defining its intensity

total sample size. At the same time, at least three trees had to show the presence of GD in a given year. Erosion intensity (erosion rate; E_r) at the edges of open cracks and trenches was calculated as the ratio of the measured distance of the sample from the perpendicular ground surface and the age (in years) of identified time of root exposure (as determined by anatomical change in the form of VLA decline).

Results

Trees and growth disturbances

In all three zones, a total of 71 trees were sampled through 142 increment cores and four exposed roots (four cross-sections). The species sampled were *F. sylvatica* (52 individuals) and *L. decidua* (19 individuals). *L. decidua* was only sampled in Zone3, where the most trees were sampled overall (43 individuals). The fewest were sampled in Zone1 (12 trees). The total age of all sampled trees was 83.9 years (stdev: 16.8 years). In general, *F. sylvatica* individuals (89.2 years; stdev: 26.9 years) were significantly (p-value from Mann–Whitney test < 0.01) older than *L. decidua* individuals (37.4 years; stdev: 2.5 years). The oldest trees were sampled in Zone2 (mean: 94.9 years; stdev: 23.7 years) and the youngest in Zone3 (mean: 64.5 years; stdev: 29.9 years). Details of the age of trees in each zone are given in Table 1. The minimum number of five living trees (the standard threshold for the relevance of the reconstructed chronology) was reached in 1922 in Zone1and 3. In Zone2, this threshold was reached in 1909 (Fig. 6). The entire logging period (since 1962) is thus fully covered by tree-ring data in all three zones.

In a total of 142 tree-ring series, 112 growth disturbances were identified, representing 1.6 GD per tree. Growth disturbances were identified only for the early harvest period (i.e., since 1962). Abrupt growth suppression generally dominated (71 cases; 63.4%) over reaction wood (41 cases; 36.6%). Details of the representation of both types of GD in each zone are given in Table 2. There was a greater difference in the relative abundance of each type of GD for both tree species. In the case of *F. sylvatica*, abrupt growth suppression was slightly more prevalent (60.0%), whereas in the case of *L. decidua*, the proportion of abrupt growth suppression was significantly higher (78.9%) at the expense of reaction wood (Fig. 7A). In the case of *F. sylvatica*, there was no difference in the duration of the two types of GDs (p-value from Mann–Whitney test = 0.58), while in the case of *L. decidua*, a significantly longer duration was found (p-value from t-test < 0. 01) for abrupt growth suppression compared to reaction wood (Fig. 7B). The intensity of GD was only detected for abrupt growth suppression and in this case no significant difference was found between the two tree species (p-value from Mann–Whitney test = 0.79; Fig. 7C).

Spatio-temporal occurrence of slope movements

Most GDs were identified in trees growing in Zone3 (66 cases). All these GDs occurred in a total of 37 years (oldest: 1964; youngest: 2021) which means a recurrence rate of 1.6 years. The threshold for determining a significant slope movement event (i.e. $I_t \geq 5\%$ and at least 3 disturbed trees at the same time) was crossed in seven years (1981, 1998, 2004, 2009, 2014, 2015, 2021; Fig. 8). The most

Table 1 Number and age of sampled trees in individual zones

Zone	Trees	Mean age (stdev)	Maximal age	Minimal age
Zone1	12	92.2 (34.8)	136	27
Zone2	16	94.9 (23.7)	136	65
Zone3	43	64.5 (29.9)	130	32
Total	71	83.9 (16.8)	136	27

Table 2 Ratio of individual GD types in all studied zones

Zone	Abrupt growth suppression (%)	Reaction wood (%)	Growth disturbances
Zone1	11 (57.9)	8 (42.1)	19
Zone2	16 (59.3)	11 (40.7)	27
Zone3	44 (66.7)	22 (33.3)	66
Total	71 (63.4)	41 (36.6)	112

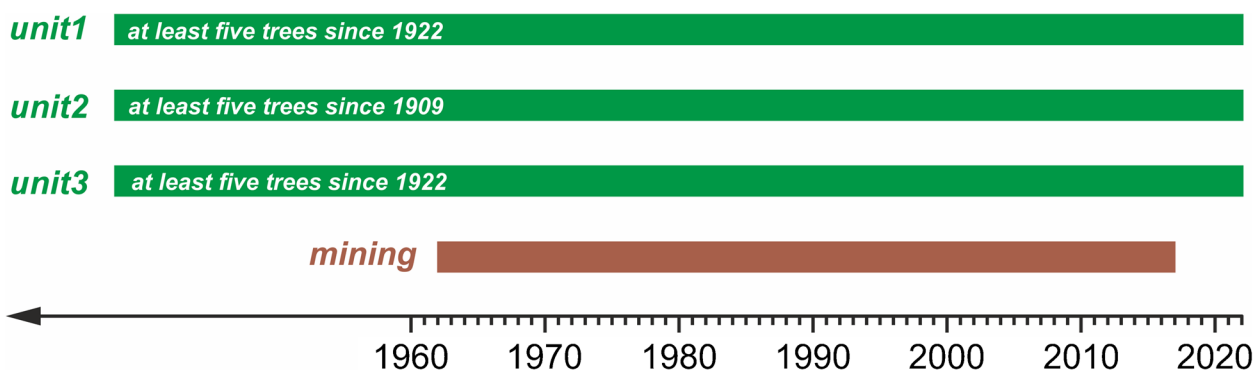


Fig. 6 Temporal overlap of tree-ring series of disturbed trees in each zone (relevant chronology is from the number of at least five living sampled trees) and the period of deep lignite mining (since 1962)

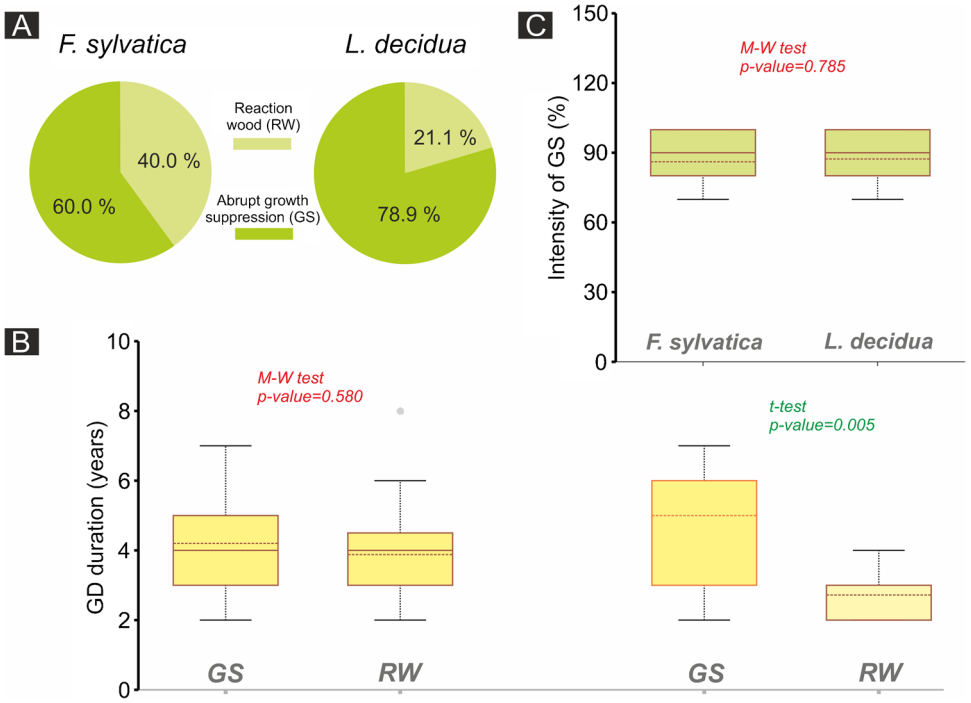


Fig. 7 Structure and properties of dated GDs induced by DSGSD movements. **A** Proportions of abrupt growth suppression and reaction wood in *F. sylvatica* and *L. decidua* specimens. **B** Differences in the duration of the two types of GDs in the two tree species studied. **C** Differences in the intensity of abrupt growth suppression in *F. sylvatica* and *L. decidua*. All differences were tested with either a non-parametric Mann–Whitney test (M-W test) or a parametric *t*-test at the $\alpha = 0.05$ significance level

pronounced events by I_t index value were in 1981 (21.7%) and 2021 (14.0%). In Zone2, 27 GDs were dated in a total of 17 years (oldest: 1969; youngest: 2019) which means a recurrence rate of 3.6 years. Significant events were detected in only 2 years (1977: $I_t = 31.3\%$ and 1981: $I_t = 37.5\%$) (Fig. 8). The fewest GDs were dated from Zone1 (19 events) and were detected in a total of 15 years (oldest: 1967; youngest: 2007) which means a recurrence rate of 4.1 years. A significant event was detected in only 1 year (1971: $I_t = 40.0\%$) when activity peaked and then declined. After 2007, no more GD was detected in this zone (Fig. 8).

The spatial distribution of the occurrence of trees with GD present in their tree-ring series during each decade is shown in Fig. 9A. The spatio-temporal decadal reconstruction corresponds to the annual chronology in each zone where Zone1 shows an increased frequency of GDs in the 1970 s and a subsequent decline in abundance to a complete absence of GDs in the last decade. In the case of Zone2, a peak in the incidence of GDs is seen during the 1970 s and 1980 s. In the last three decades, the number of dated GDs is low. In Zone3, a peak in the occurrence of GDs during the 1980 s and then a recent increase in abundance in the last decade is visible (Fig. 9A). Figure 9B shows parts of each zone with a long-term higher frequency of GDs. Within Zone1, this is the middle part. In the case of Zone2, it is its northern edge, and in the case of Zone3, it is its northern edge.

The intensity of erosion at the edges of open tension cracks and trenches was studied by dating the anatomical responses in four tree roots to their exposure (just the effect of erosion at the edges of the forms studied). Two roots were analyzed in Zone1 and 2 roots in Zone2 (Fig. 9C). The age of the roots was between 45 and 57 years and their sudden exposure occurred between 1975 and 1985. Based on the distance of the root from the total ground surface, the erosion rate was calculated and ranged between 0.9 and 3.2 cm.year^{-1}. Generally higher erosion rate values were found in Zone1 than in Zone3 (Fig. 9C). Details of the ages of the analyzed roots and the calculated erosion rate values are given in Table 3.

Discussion

This study analyzed a tree-ring series of 71 disturbed trees affected by recent DSGSD development. Erosion rates of fresh edges of trenches and tension cracks were reconstructed by dendrochronological dating of anatomical responses of exposed tree roots. Chronological data from two tree species (*F. sylvatica* and *L. decidua*) revealed distinct spatio-temporal evolution of the studied DSGSD in three subzones.

Growth responses of trees to DSGSD movements

Both *F. sylvatica* and *L. decidua* are species that are commonly used for dendrogeomorphic dating of various types of slope processes (Stoffel et al. 2005; Van Den Van Den Eeckhaut et al. 2009). However, differences in the anatomical structure of the two species appear to have caused the different nature of the detected GDs in their tree-ring series. The movement of the blocks was with minimal rotation, which in other types of slope processes is responsible for the strong

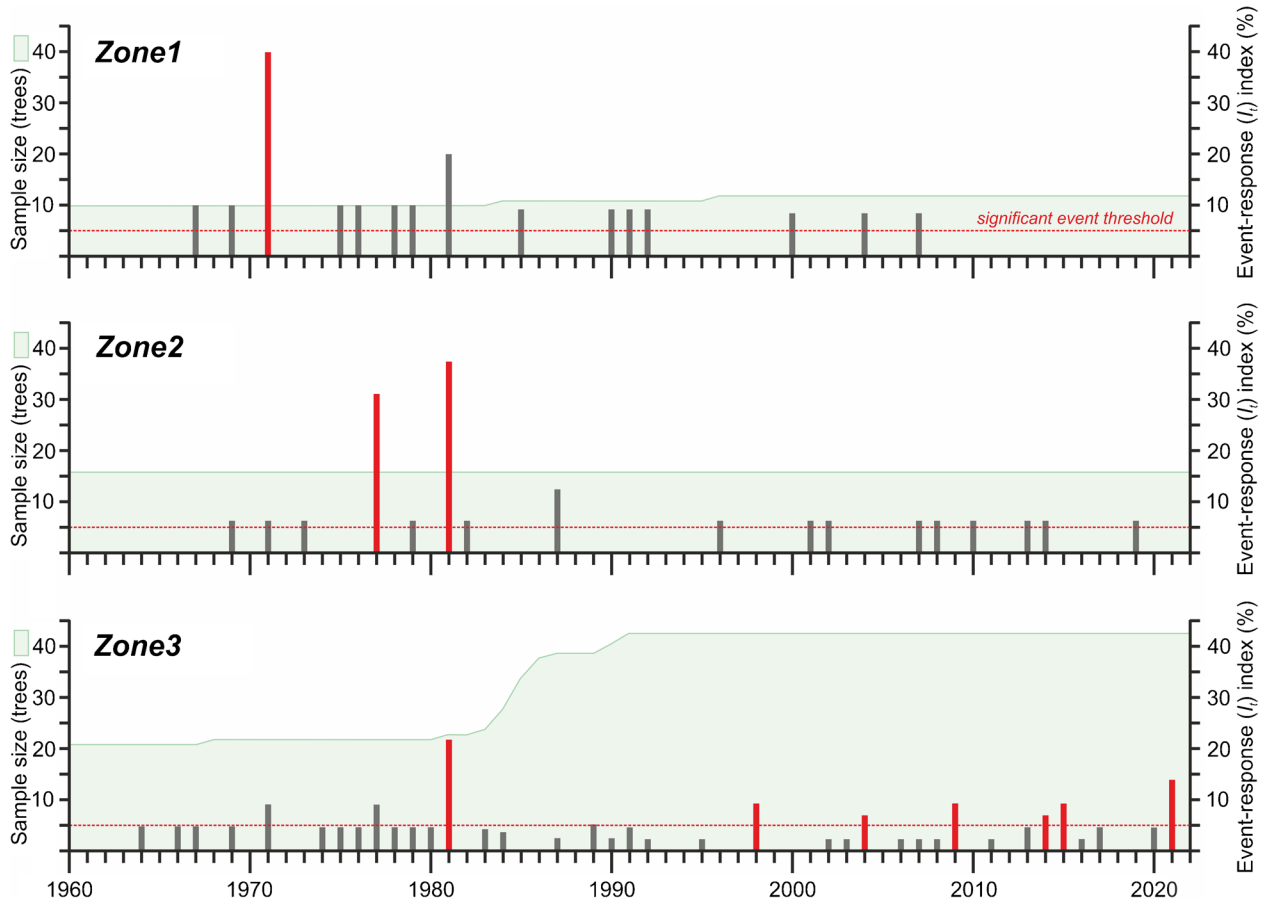


Fig. 8 Annual chronology of DSGSD activity movements expressed using the event-response (I_t) index including chronological evolution of sample size. The threshold for defining a significant event is $I_t \geq 5\%$ and also at least three disturbed trees

tilting of tree trunks (Šilhán 2021). In the case of this study, however, the tilting of the trunks was only due to the specific position of the trees at the interface of the two blocks, where the resulting differences in drop height deflected the trunks from their vertical position. At the same time, the movement at the block interface caused strong tensile and shearing effects on the roots. Thus, the dominant growth responses of the trees took the form of abrupt growth suppression (response to root damage) and reaction wood (response to trunk lean). However, there was a significant difference in the abundance of both types of GD between the two species.

In terms of potential differences in GD type between the two tree species, they are mainly based on the different structure of the root systems. *L. decidua* is characterized by the development of one deep central root (Chalupa 1991; Dorren et al. 2005), which ensures the stability of the trunk. If this is damaged, growth is severely stunted. This response may be stronger than in the case of damage to multiple sub-roots in species with a more branched system. The central root in *L. decidua* provides point stability to the trunk, which appears to be an effective feature in the case of DSGSD sub-block movements because the trunk condition is not as affected by the vertical differences of the two rock blocks. This only was fully reflected in the proportion of both types of GD, with abrupt growth suppression fully dominating over reaction wood. Damage to the root system in trees leads to stress (due to insufficient water and nutrient supply), which is then reflected in the tree trunk by a sudden reduction in tree-ring widths, in this case referred to as abrupt growth suppression. In addition, this effect probably had an influence on the longer duration of abrupt growth suppression compared to reaction wood. It is possible to trace a difference from the influence of landslide movements, where abrupt growth suppression is the most common type of GD in shallow landslides with numerous internal deformations (Lopez Saez et al. 2012), whereas it is minimally found in rotational movements of compact landslide blocks (Šilhán et al. 2013).

In contrast, *F. sylvatica* has a more branched root system that stabilizes the trunk by anchoring in the near-surface soil and weathering mantle (Mainiero and Kazda 2006). Thus, individuals of *F. sylvatica* growing at the interface of two blocks with different drop sizes are easily tilted even without the rotational mechanism of slope movement. This tilting appears to be a stronger stimulus than damage to the broad root system in many cases. Reaction wood formation thus occurs in a higher proportion than in *L. decidua*. Also in the case of *F. sylvatica*, the specificity of DSGSD movements was evident. Indeed, similar damage to the root system can occur during creep movements, when the trunk is also less intensely tilted and abrupt growth suppression dominates. However, even in the case of greater trunk tilt, more pronounced root damage dominates the effect on the resulting growth response.

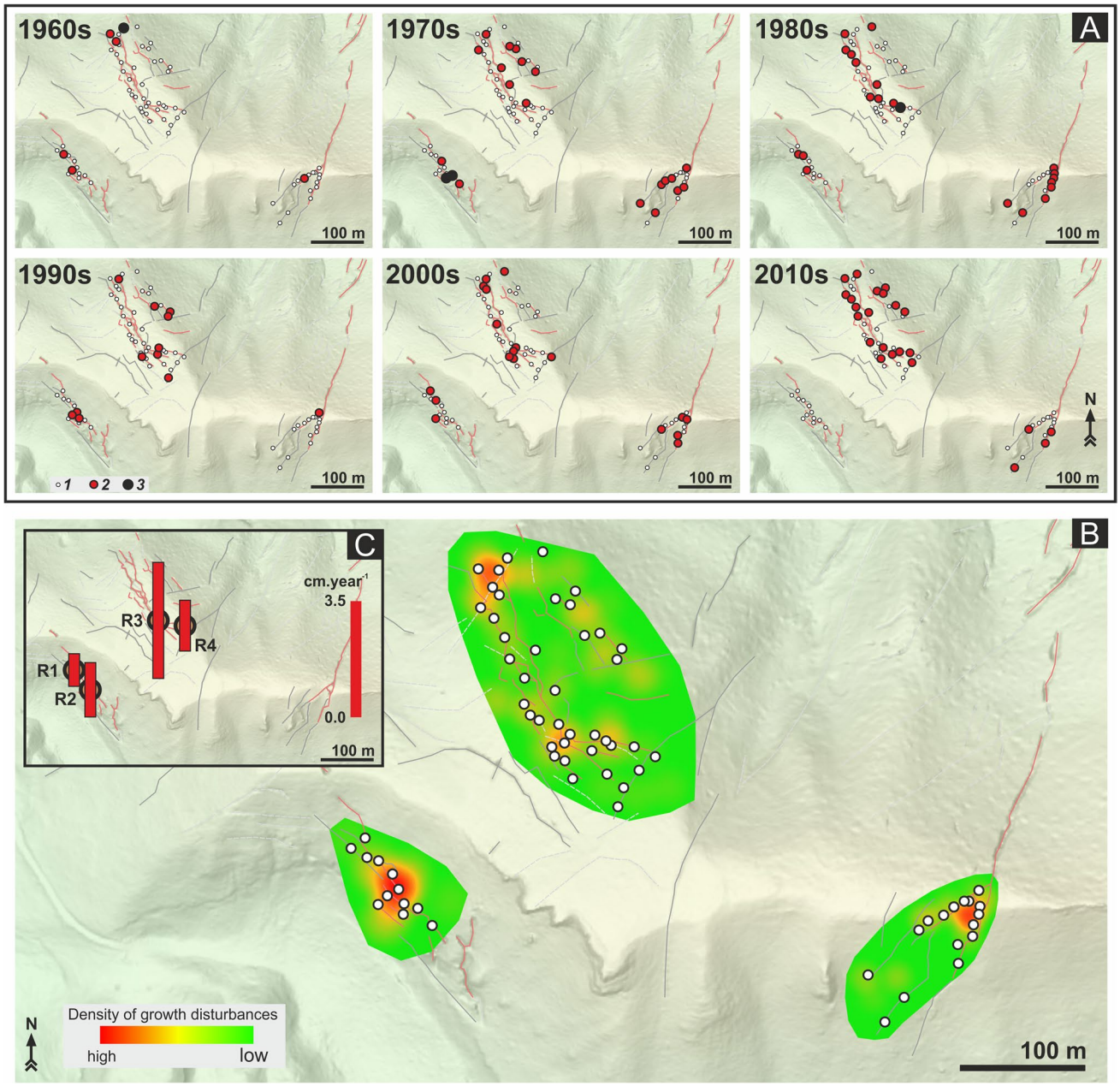


Fig. 9 Spatio-temporal reconstruction of DSGSD movements and erosion rate. **A** Decadal spatial distribution of trees with growth disturbances (1—position of sampled trees, 2—tree with one GD, 3—tree with two GD). **B** Spatial density of GDs. **C** Spatial distribution of erosion rate values

Spatio-temporal evolution of the studied DSGSD

The present study offers a unique insight into the initial stages of DSGSD evolution, which are usually radiometrically dated with some degree of uncertainty (Hermanns et al. 2013; Zerathe et al. 2013). The recent (on the order of decades) evolution of DSGSD is quite dominantly detected by various monitoring methods (Klimeš et al. 2012). Due to the knowledge of the history of the underlying factor that triggered the initiation and evolution of DSGSD (the beginning of deep mining in 1962) it was possible to use tree-ring series to completely cover the period of initial failure and its subsequent evolution, which is unique result at annual resolution. The trigger of the entire DSGSD is attributed to the process associated with deep lignite mining within Tertiary sedimentary formations, coupled with the occurrence of lava outflows present on the surface of the terrain. The observed deformation morphology in the form of open trenches confirms the assumption of Agliardi et al. (2001) about the presence of shear surfaces and does not support the view of Dramis and Sorriso-Valvo (1994), who do not assume the presence of these structures.

Table 3 Exposed roots-based erosion parameters of open crack edges

Root	Age (years)	Distance from ground (cm)	Exposure year	Erosion rate (cm. year^{-1})
R1	57	43	1975	0.9
R2	52	68	1977	1.5
R3	45	120	1985	3.2
R4	49	57	1982	1.4

The reconstructed spatio-temporal evolution of the studied DSGSD combined with the observed block displacements is inconsistent with the general pattern of deformation evolution in the form of gradual creep and subsequent partial reactivations on the order of tenths of a mm per year (Pánek and Klimeš 2016). The specificity of the triggering factor (anthropogenic mining) combined with the presence of volcanic complexes in the overburden may influence this divergence. The observed movements must have had an average intensity of up to several tens of cm per year, taking into account the overall displacement values. This raises the question of potential catastrophic reactivation of the DSGSD (Chigira et al. 2010). However, the magnitude of initial failure may have been comparable to recent examples that have not yet been catastrophically reactivated. For example, Brueckl and Parotidis (2001) documented the sudden emergence of up to 3 m of slope, or Jibson et al. (2004) recorded the emergence of up to 5-m-high step after an earthquake. The nature of the initial failure in the form of high-magnitude motion is also suggested by tree-ring based data. For each of the three sub-study zones, it is evident that smaller movements (affecting only a limited number of trees) began to occur after a short period from the start of mining, after which the largest event in the zone always occurred (1971 and 1981 in Zone1; 1977 and 1981 in Zone2; 1981 in Zone2). After this event, the movements then tend to be more of a fade-out (typical for zone1), except for Zone3, where a gradual recovery of movements is evident in recent years. The continuous to recent activity in Zone3 may also explain the average lowest tree age in this zone. Increased activity may gradually prevent trees from reaching a higher age due to damage that causes them to die more often than in less active zones. Overall, however, this pattern of evolution is consistent with the general assumptions of DSGSD evolution, albeit in a strongly time-accelerated scenario. This can be attributed to the specificities (anthropogenic and lithological) of the study site.

The current state of the studied DSGSD has clear morphologically fresh surface features in the form of open cracks and trenches. The existence of extensive crevice-type caves below the surface can even be expected especially because of the intense exhalations of very cold air were observed at the open entrances to the underground spaces. However, the recent evolution also suggests a considerable dynamic modelling of this relief. Based on the dating of anatomical changes (1970 s–80 s) in the exposed roots of trees growing on the margins of open fissures and trenches, it is clear that erosional processes began immediately after the formation of these forms at initial failure. Considering the reconstructed erosion rate (even more than 3 cm.year^{-1}), it is clear that the initial fresh morphology will be very smoothed over several tens to hundreds of years (if no further revival of movements occurs in the post-logging period). Moreover, the rapidity (suddenness) of the anatomical response in the roots clearly confirms the high erosion rate, because exposure must occur rapidly (Stoffel et al. 2013b) and high annual losses of slope material can be expected.

Conclusions

This study provides the first dendrogeomorphic real dating of DSGSD movements in the World. In doing so, it takes advantage of the unique opportunity to apply tree-ring based methods to a site where DSGSD formation is anthropogenically induced by the influence of deep mining that began in 1962, and this entire period is covered by tree-ring data. The studied DSGSD was divided into three separate morphological zones and each was studied separately using 142 tree-ring series from 71 trees (53 individuals of *F. sylvatica* and 19 individuals of *L. decidua*). The structure of the growth disturbance induced by DSGSD movement is similar to that induced by landslide movements, however, there are significant specificities between the two species, which probably result from the different morphologies of the root systems. The constructed movement chronology reveals the evolution of DSGSD from initial failure to subsequent attenuation of movements to their current reactivation in the easternmost part of the slope where the extensive open crack across the entire ridge was developed. Anatomical analyses of exposed tree roots growing on the edges of open cracks and trenches revealed their dynamic evolution with high erosion rates modeling them. The study thus provides a unique retrospective analysis of the recent evolution of DSGSD over the past decades. However, as with the application of the tree-ring based approach to other slope movement types, the inertia of growth disturbances is a key issue in dating high frequency events. Thus, future research should aim to minimize this aspect of dendrogeomorphic research.

Acknowledgements

The authors thank Hornonitrianske mines Prievidza a.s. for providing information on underground mining.

Funding

Open access publishing supported by the institutions participating in the CzechELib Transformative Agreement. The Czech Science Foundation project no. 22-12522S, Slovak Research and Development Agency ("APVV") APVV-22–0024, and Scientific Grant Agency of the Ministry of Education, Science, Research and Sport of the Slovak Republic and the Slovak Academy of Sciences ("VEGA") No. 1/0217/23 supported this study.

Data availability

Data will be available upon request.

Declarations

Competing interests The authors declare no competing interests.

Open Access This article is licensed under a Creative Commons Attribution 4.0 International License, which permits use, sharing, adaptation, distribution and reproduction in any medium or format, as long as you give appropriate credit to the original author(s) and the source, provide a link to the Creative Commons licence,

and indicate if changes were made. The images or other third party material in this article are included in the article's Creative Commons licence, unless indicated otherwise in a credit line to the material. If material is not included in the article's Creative Commons licence and your intended use is not permitted by statutory regulation or exceeds the permitted use, you will need to obtain permission directly from the copyright holder. To view a copy of this licence, visit http://creativecommons.org/licenses/by/4.0/.

References

Agliardi F, Crosta G, Zanchi A (2001) Structural constraints on deep-seated slope deformation kinematics. Eng Geol 59:83–102. https://doi.org/10.1016/S0013-7952(00)00066-1

Alestalo J (1971) Dendrochronological interpretation of geomorphic processes. Fennia 105:1–139

Ambrosi C, Crosta GB (2006) Large sackung along major tectonic features in the Central Italian Alps. Eng Geol 83:183–200. https://doi.org/10.1016/j.enggeo.2005.06.031

Bigot-Cormier F, Braucher R, Bourles D et al (2005) Chronological constraints on processes leading to large active landslides. Earth Planet Sci Lett 235:141–150. https://doi.org/10.1016/j.epsl.2005.03.012

Blair RW (1994) Moraine and valley wall collapse due to rapid deglaciation in Mount Cook National Park. New Zealand Mt Res Dev 14:347. https://doi.org/10.2307/3673731

Bochníček O, Bosányi P, Čepčeková E et al (2015) Climate Atlas of Slovakia. Slovenský hydrometeorologický ústav, Bratislava

Brueckl E, Parotidis M (2001) Estimation of large-scale mechanical properties of a large landslide on the basis of seismic results. Int J Rock Mech Min Sci 38:877–883. https://doi.org/10.1016/S1365-1609(01)00053-3

Butler DR, Malanson GP, Oelfke JG (1987) Tree-ring analysis and natural hazard chronologies: minimum sample sizes and index values. Prof Geogr 39. https://doi.org/10.1111/j.0033-0124.1987.00041.x

Chalupa V (1991) Larch (Larix decidua Mill.). In: Bajaj YPS (ed) Trees III. Springer, Berlin Heidelberg, pp 446–470

Chigira M, Wu X, Inokuchi T, Wang G (2010) Landslides induced by the 2008 Wenchuan earthquake, Sichuan, China. Geomorphology 118:225–238. https://doi.org/10.1016/j.geomorph.2010.01.003

Čičmanec P, Bražina M, Šarkan J (2009) Final report with reserves calculation, exclusive deposit Handlová, mining area Cigeľ

Clague JJ, Souther JG (1982) The Dusty Creek landslide on Mount Cayley, British Columbia. Can J Earth Sci 19:524–539

Cook ER (1983) A time series analysis approach to tree-ring standardization. University of Arizona, Tucson

Corona C, Lopez Saez J, Stoffel M (2014) Defining optimal sample size, sampling design and thresholds for dendrogeomorphic landslide reconstructions. Quat Geochronol 22:72–84. https://doi.org/10.1016/j.quageo.2014.02.006

Crosta GB, Frattini P, Agliardi F (2013) Deep seated gravitational slope deformations in the European Alps. Tectonophysics 605:13–33. https://doi.org/10.1016/j.tecto.2013.04.028

Czikhardt R, Papco J, Bakon M et al (2017) Ground stability monitoring of undermined and landslide prone areas by means of Sentinel-1 multitemporal InSAR, case study from Slovakia. Geosciences (Basel) 7:87. https://doi.org/10.3390/geosciences7030087

Dorren LKA, Berger F, le Hir C et al (2005) Mechanisms, effects and management implications of rockfall in forests. For Ecol Manage 215:183–195. https://doi.org/10.1016/j.foreco.2005.05.012

Dramis F, Sorriso-Valvo M (1994) Deep-seated gravitational slope deformations, related landslides and tectonics. Eng Geol 38:231–243. https://doi.org/10.1016/0013-7952(94)90040-X

Fantucci R, Sorriso-Valvo M (1999) Dendrogeomorphological analysis of a slope near Lago, Calabria (Italy). Geomorphology 30:165–174. https://doi.org/10.1016/S0169-555X(99)00052-5

Gärtner H (2007) Tree roots - Methodological review and new development in dating and quantifying erosive processes. Geomorphology 86:243–251. https://doi.org/10.1016/j.geomorph.2006.09.001

Gärtner H, Nievergelt D (2010) The core-microtome: a new tool for surface preparation on cores and time series analysis of varying cell parameters. Dendrochronologia (Verona) 28:85–92

Gärtner H, Lucchinetti S, Schweingruber FH (2014) New perspectives for wood anatomical analysis in dendrosciences: the GSL1-microtome. Dendrochronologia (Verona) 32:47–51. https://doi.org/10.1016/j.dendro.2013.07.002

Hermanns R, Oppikofer T, Dahle H et al (2013) Understanding long-term slope deformation for stability assessment of rock slopes: the case of the Oppstadhornet rockslide, Norway. Ital J Eng Geol Environ 255–264. https://doi.org/10.4408/IJEGE.2013-06.B-23

Holmes R (1983) Computer-assisted quality control in tree-ring dating and measurement. Tree-Ring Bull 43:69–73

Hughes PD, Gibbard PL, Ehlers J (2013) Timing of glaciation during the last glacial cycle: evaluating the concept of a global 'last glacial maximum' (LGM). Earth Sci Rev 125:171–198. https://doi.org/10.1016/j.earscirev.2013.07.003

Jibson RW, Harp EL, Schulz W, Keefer DK (2004) Landslides triggered by the 2002 Denali Fault, Alaska, earthquake and the inferred nature of the strong shaking. Earthq Spectra 20:669–691. https://doi.org/10.1193/1.1778173

Klimeš J, Rowberry MD, Blahůt J et al (2012) The monitoring of slow-moving landslides and assessment of stabilisation measures using an optical–mechanical crack gauge. Landslides 9:407–415. https://doi.org/10.1007/s10346-011-0306-4

Leonelli G, Chelli A, Consonni M et al (2020) Multi-decadal dating of surface slope movements in forested DSGSD areas of the European Alps: detecting precipitation triggers factors. Geografiska Annaler Ser A Phys Geogr:1–25. https://doi.org/10.1080/04353676.2020.1813983

Lopez Saez J, Corona C, Stoffel M et al (2012) Probability maps of landslide reactivation derived from tree-ring records: Pra Bellon landslide, southern French Alps. Geomorphology 138:189–202. https://doi.org/10.1016/j.geomorph.2011.08.034

Mainiero R, Kazda M (2006) Depth-related fine root dynamics of Fagus sylvatica during exceptional drought. For Ecol Manage 237:135–142. https://doi.org/10.1016/j.foreco.2006.09.034

Maxwell RS, Larsson L-A (2021) Measuring tree-ring widths using the CooRecorder software application. Dendrochronologia (Verona) 67:125841. https://doi.org/10.1016/j.dendro.2021.125841

Moro M, Saroli M, Salvi S et al (2007) The relationship between seismic deformation and deep-seated gravitational movements during the 1997 Umbria–Marche (Central Italy) earthquakes. Geomorphology 89:297–307. https://doi.org/10.1016/j.geomorph.2006.12.013

Němčok A (1982) Landslides in Slovak Carpathians. Veda Publishers, Slovak Academy of Sciences, Bratislava

Pánek T (2015) Recent progress in landslide dating: global overview. Prog Phys Geogr 39:168–198

Pánek T, Klimeš J (2016) Temporal behavior of deep-seated gravitational slope deformations: a review. Earth Sci Rev 156:14–38. https://doi.org/10.1016/j.earscirev.2016.02.007

Pánek T, Lenart J, Hradecký J et al (2018) Coastal cliffs, rock-slope failures and late quaternary transgressions of the Black Sea along southern Crimea. Quat Sci Rev 181. https://doi.org/10.1016/j.quascirev.2017.12.004

Rubiales JM (2008) Response of Pinus sylvestris roots to sheet-erosion exposure: an anatomical approach. Nat Hazard 8:223–231. https://doi.org/10.5194/nhess-8-223-2008

Schweingruber FH (1978) Mikroskopische Holzanatomie. Swiss Federal Institute of Forestry Research, Birmensdorf

Schweingruber FH, Eckstein D, Serre-Bachet F, Bräker OU (1990) Identification, presentation and interpretation of event years and pointer years in dendrochronology. Dendrochronologia (Verona) 8:9–38

Shroder JF (1978) Dendrogeomorphological analysis of mass movement on Table Cliffs Plateau, Utah. Quat Res 9:168–185. https://doi.org/10.1016/0033-5894(78)90065-0

Shroder JF, Owen LA, Seong YB et al (2011) The role of mass movements on landscape evolution in the Central Karakoram: discussion and speculation. Quatern Int 236:34–47. https://doi.org/10.1016/j.quaint.2010.05.024

Šilhán K (2020) Dendrogeomorphology of landslides: principles, results and perspectives. Landslides 17:2421–2441. https://doi.org/10.1007/s10346-020-01397-4
Šilhán K (2021) Dendrogeomorphology of different landslide types: a review. Forests 12:1–19
Šilhán K, Pánek T, Dušek R et al (2013) The dating of bedrock landslide reactivations using dendrogeomorphic techniques: the Mazák landslide, Outer Western Carpathians (Czech Republic). Catena (Amst) 104:1–13. https://doi.org/10.1016/j.catena.2012.12.010
Šilhán K, Pánek T, Škarpich V (2022) Diversification of landslide areas as a means for reducing noise in dendrogeomorphic dating. Quat Geochronol 72:101362. https://doi.org/10.1016/j.quageo.2022.101362
Šimon L, Elečko M, Lexa J et al (1997) Geological map of the Vtacnik Mts. and Upper Nitra Depression, 1:50,000. Bratislava
Stoffel M, Bollschweiler M (2008) Tree-ring analysis in natural hazards research - an overview. Nat Hazard 8:187–202. https://doi.org/10.5194/nhess-8-187-2008
Stoffel M, Schneuwly D, Bollschweiler M et al (2005) Analyzing rockfall activity (1600–2002) in a protection forest - a case study using dendrogeomorphology. Geomorphology 68:224–241. https://doi.org/10.1016/j.geomorph.2004.11.017
Stoffel M, Butler DR, Corona C (2013a) Mass movements and tree rings: a guide to dendrogeomorphic field sampling and dating. Geomorphology 200:106–120. https://doi.org/10.1016/j.geomorph.2012.12.017
Stoffel M, Corona C, Ballesteros JA, Bodoque JM (2013b) Dating and quantification of erosion processes based on exposed roots. Earth Sci Rev 123:18–34. https://doi.org/10.1016/j.earscirev.2013.04.002
Timell TE (1986) Compression wood in gymnosperms, 1st edn. Springer Berlin Heidelberg, Berlin
Van Den Eeckhaut M, Muys B, Van Loy K et al (2009) Evidence for repeated re-activation of old landslides under forest. Earth Surf Process Landf 34:352–365. https://doi.org/10.1002/esp.1727
Vandekerckhove L, Muys B, Poesen J et al (2001) A method for dendrochronological assessment of medium-term gully erosion rates. Catena (Amst) 45:123–161. https://doi.org/10.1016/S0341-8162(01)00142-4
Westing AH (1965) Formation and function of compression wood in gymnosperms II. Bot Rev 34:51–78
Zerathe S, Braucher R, Lebourg T et al (2013) Dating chert (diagenetic silica) using in-situ produced 10Be: possible complications revealed through a comparison with 36Cl applied to coexisting limestone. Quat Geochronol 17:81–93. https://doi.org/10.1016/j.quageo.2013.01.003
Zhang Y, Stoffel M, Liang E et al (2019) Centennial-scale process activity in a complex landslide body in the Qilian Mountains, northeast Tibetan Plateau, China. Catena (Amst) 179:29–38

Publisher's Note Springer Nature remains neutral with regard to jurisdictional claims in published maps and institutional affiliations.

Karel Šilhán (✉)
Department of Physical Geography and Geoecology, University of Ostrava, Chittussiho 10, Ostrava – Slezská Ostrava, Czech Republic
Email: karel.silhan@osu.cz

Ivan Ružek
Department of Physical Geography and Geoinformatics, Comenius University in Bratislava, Ilkovičova 6, Bratislava 4, Slovakia